Arch. Pharm. Chem. Life Sci. 2015, *348*, 1–15

ARCH PHARM
Archiv der Pharmazie

Full Paper

Vitamin D Analogue: Potent Antiproliferative Effects on Cancer Cell Lines and Lack of Hypercalcemic Activity

María Julia Ferronato[1], Débora Gisele Salomón[1], María Eugenia Fermento[1], Norberto Ariel Gandini[1], Alejandro López Romero[2], Marcos Lois Rivadulla[3], Xenxo Pérez-García[3], Generosa Gómez[3], Manuel Pérez[3], Yagamare Fall[3], María Marta Facchinetti[1], and Alejandro Carlos Curino[1]

[1] Laboratorio de Biología del Cáncer, Instituto de Investigaciones Bioquímicas Bahía Blanca (INIBIBB-CONICET), Centro Científico Tecnológico Bahía Blanca, Bahía Blanca, Argentina
[2] Departamento de Hematología, Laboratorios IACA, Bahía Blanca, Argentina
[3] Departamento de Química Orgánica, Facultad de Química, Instituto de Investigación Biomedica (IBI), Universidad de Vigo, Vigo, Spain

The active form of vitamin D_3, $1\alpha,25(OH)_2D_3$, plays a major role in maintaining calcium/phosphate homeostasis. In addition, it is a potent antiproliferative and pro-differentiating agent. Unfortunately, it usually causes hypercalcemia *in vivo* when effective antitumour doses are used. It has therefore been found necessary to synthesise new analogues that retain or even increase the antitumour effects but preclude hypercalcemia. This report presents the synthesis of a novel Gemini vitamin D analogue (UVB1) and its biological evaluation. We demonstrate that this compound has potent antitumoural effects over a wide panel of tumour cell lines while showing lack of hypercalcemic activity and toxicity effects in *in vivo* assays.

Keywords: Antiproliferative agents / Antitumour activity / Cancer treatment / Cell line / Gemini

Received: December 4, 2014; Accepted: February 27, 2015

DOI 10.1002/ardp.201400448

Additional supporting information may be found in the online version of this article at the publisher's web-site.

Introduction

The hormonally active metabolite of vitamin D_3, $1\alpha,25$-dihydroxyvitamin D_3 ($1\alpha,25(OH)_2D_3$, calcitriol), is known to play a major role in maintaining calcium/phosphate homeostasis. In addition, it is important for the inhibition of cell proliferation, induction of apoptosis and increased cell differentiation in cancer cells, all processes involved in the inhibition of tumour progression. These potent growth-inhibitory properties make calcitriol an ideal compound to treat hyperproliferative disorders such as cancer. However, its severe hypercalcemic effects have severely hampered its therapeutic application. One way to overcome this problem is to design structural analogues of calcitriol with the same or even increased antitumour effects and with reduced undesired effects on calcium and bone metabolism.

Several analogues have been synthesised and tested in various cell lines and animal models, in some cases with promising results [1–3]. Despite its interesting antitumoural effects, a small number of single agent trials utilising vitamin D_3 analogues have been conducted [3]. The large majority of the analogues have been obtained by modifying the side chain [4, 5]. However, most agonists carry only minor modifications compared with the natural hormones [6]. A remarkable exception is Gemini, which is the first $1\alpha,25(OH)_2D_3$ analogue that carries two side chains [7–10], thereby increasing ~25% the volume of the natural hormone.

This report describes the synthesis and the biological evaluation of a novel Gemini vitamin D analogue (UVB1). For the biological assays, the effects of this analogue on proliferation, apoptosis and migration were assessed on

Correspondence: Dr. Alejandro C. Curino, Laboratorio de Biología del Cáncer, Instituto de Investigaciones Bioquímicas Bahía Blanca (INIBIBB-CONICET), Centro Científico Tecnológico Bahía Blanca, Camino La Carrindanga Km 7-C.C. 857, Bahía Blanca 8000, Argentina.
E-mail: acurino@criba.edu.ar
Fax: +54-291-4861200

different cancer cell lines and the calcemic activity was evaluated in mice.

Results

Synthesis

We have recently developed a new and efficient synthetic methodology for the preparation of Gemini vitamin D analogues [11]. This procedure involves a key chemical transformation (a sigmatropic rearrangement) that provides great versatility and selectivity in the synthesis of this type of compounds. Previous synthetic methods have relied on the non-selective generation of the double side chain precursor and subsequent separation of isomers, thus requiring the use of expensive and time-consuming chromatography techniques such as HPLC. Our method has allowed us to synthesize Gemini analogue Ro-438-3582 [10, 11], and a new Gemini analogue UVB1 which was obtained serendipitously (Fig. 1).

Scheme 1 shows the initial approach we designed for the synthesis of Ro-438-3582. Ketone **1**, easily prepared from Inhoffen diol [12] was the precursor of alkene **2** [11] which was hydrogenated over Pd/C to afford ester **3**. Dibal reduction of **3** afforded alcohol **4** together with aldehyde **5**. TPAP oxidation of alcohol **4** gave aldehyde **5** in good yields. Aldehyde **5** underwent an Ohira–Bestmann homologation [13] to give alkyne **7**. Selective deprotection of the primary hydroxyl group of **7** afforded alcohol **8** which was easily converted into iodide **9**.

We anticipated that a nickel-mediated conjugate addition of iodide **9** to methyl acrylate [14, 15] would afford ester **11**, the precursor of Ro-438-3582. However, the outcome of this reaction was rather surprising. Indeed the expected ester **11** was obtained, together with diester **10**. The mechanistic rationale for the formation of ester **10** is yet to be determined. Nevertheless, as we serendipitously synthesised ester **10** we thought it might lead to a potentially interesting new Gemini analogue which we called UVB1. Accordingly, **10** on reaction with methyllithium afforded diol **12** which underwent a deprotection of its hydroxyl group, followed by a PDC oxidation and TMS protection of the side chains hydroxyl groups, giving ketone **13**. The Wittig–Horner reaction of ketone **13** with the anion derived from the phosphine oxide **14** [16, 17], followed by removal of the silyl protecting groups afforded targeted Gemini analogue UVB1.

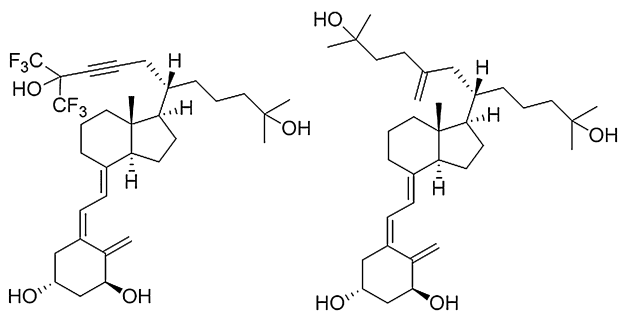

Figure 1. Structures of two analogues of Gemini: Ro-438-3582 and UVB1.

Biological evaluation

Effects of UVB1 analogue on cell count

In order to test the biological activity of the Gemini analogue UVB1, we first analysed the effects of this compound on cell count of various cancer cell lines. In preliminary testing, we performed dose- and time-course response experiments (0–120 h) in human glioblastoma multiforme (U251) and head and neck squamous cell carcinoma (HN13) cell lines with different concentrations of UVB1 (0.01–100 nM) (Fig. 2). Although a significant decrease in cell number was observed at 96 h with doses of 10 and 100 nM, further treatments were carried out at 120 h because at this time point most drug concentrations (0.01–100 nM in HN13 cell line and 10–100 nM in U251 cell line) showed effects on cell count.

Cellular viability was also confirmed by WST assays, obtaining similar results to those obtained with cell count (Supporting Information Figure S1).

Based on these results, we performed dose–response analyses at 120 h in a wide panel of cell lines, comparing the effects of UVB1 with those elicited by the natural hormone calcitriol.

As shown in Fig. 3, we observed a significant decrease in cell count after treatment with UVB1 in the human colorectal cancer HCT116 (A), human glioblastoma U251 (B), human head and neck squamous cell carcinoma HN13 (D) and HN12 (E) and human breast adenocarcinoma T47D (F) cell lines. Furthermore, in U251 and in HN13 cell lines, the reduction in cell number caused by UVB1 was greater than that elicited by calcitriol.

Table 1 shows the half maximal inhibitory concentration (IC_{50}) of the cell lines that responded to UVB1 treatments. In HN12 cells, the antiproliferative effect caused by UVB1 was similar to that elicited by calcitriol. The half maximal inhibitory concentration (IC_{50}) was 0.071 and 0.084 nM for UVB1 and calcitriol, respectively. In HN13 and U251 cell lines, the effect on cell number of UVB1 was more potent than calcitriol. In contrast, no effect was observed in the human glioma T98G (C) and murine hormone-insensitive breast adenocarcinoma LM3 (G) cell lines.

Considerable variation in the antitumour response to analogues has been observed among different types of cells and different types of tumours. The differential response of tumour cells to analogues is largely unknown and might be explained by differences in analogue binding to the vitamin D receptor (VDR) or to vitamin D-binding protein (DBP), by the different level of interaction of the VDR with co-activators upon analogue binding, or by differences in the compound metabolism [1, 18–20]. Although CYP24A1 enzyme is located primarily in the liver, it was shown to be expressed by many

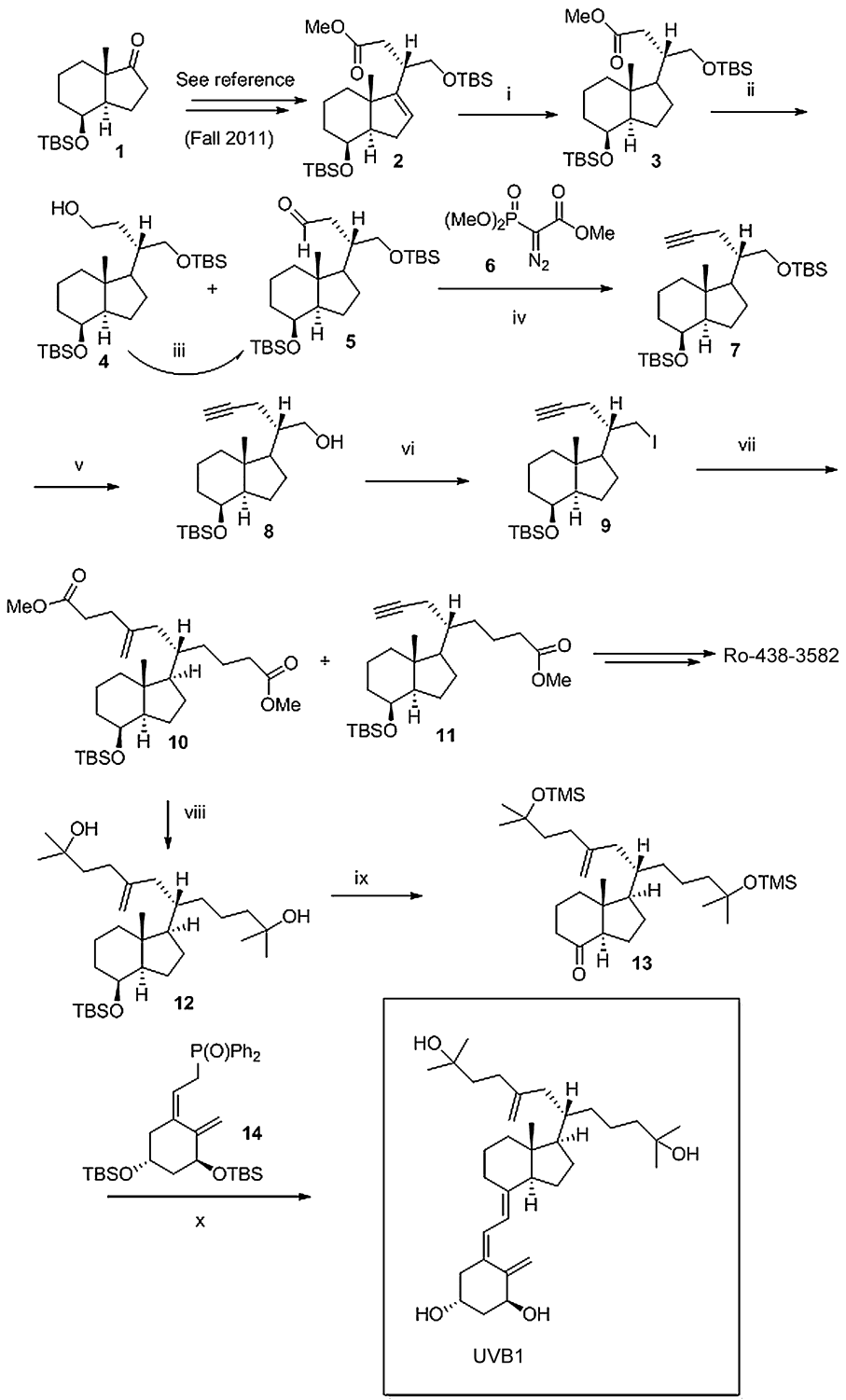

Scheme 1. Reagents and conditions. (i) H_2, Pd/C, EtOAc (98%); (ii) Dibal-H, hexane, (**4**, 73% and **5**, 20%); (iii) TPAP, NMO, CH_2Cl_2 (90%); (iv) **6**, K_2CO_3, MeOH, 0°C to rt (61%); (v) TBAF, THF (99%); (vi) I_2, PPh_3, Im, THF (77%); (vii) methyl acrylate, $NiCl_2 \cdot 6H_2O$, Zn, Pyr (**10**, 40% and **11**, 42%); (viii) MeLi, THF (99%); (ix) a) TBAF, THF; b) PDC, CH_2Cl_2; c) TMS-Im (64%, 3 steps; (x) a) **14**, *n*-BuLi, THF, −78°C, b) TBAF, THF (70%, 2 steps).

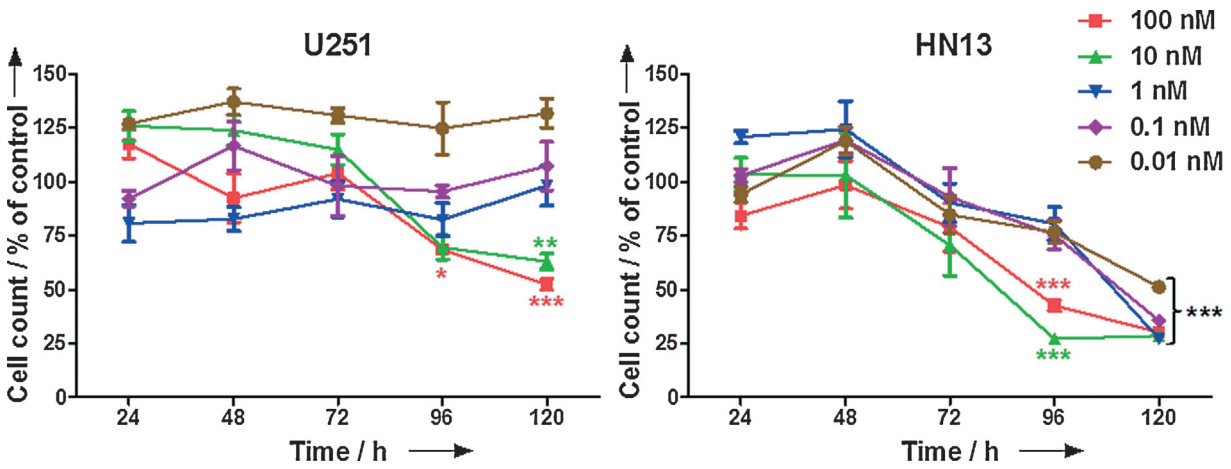

Figure 2. Time-course response analysis of UVB1 on cell count of human glioblastoma multiforme U251 and head and neck squamous cell carcinoma HN13 cell lines. Cells were exposed to the indicated concentrations (nM) of UVB1 analogue over a total period of 120 h. Cell count was expressed as percentage of the vehicle-treated cells. Data points represent means ± SD from four replicates. The experiment was repeated twice for each cell line. *p* values from Bonferroni post test of ANOVA analysis are shown. $^{*}p < 0.05$, $^{**}p < 0.01$ and $^{***}p < 0.001$ with respect to vehicle.

tissues [19]. Augmented expression of CYP24A1 has proved to be detrimental to calcitriol antiproliferative effects. Indeed, in prostate cancer cell lines, it has been demonstrated that enzyme expression inversely correlated with the antiproliferative effects displayed by the cells [21]. In this regard, Gemini analogues may be degraded by cells displaying high expression of CYP24A1, which could account for the lack of activity observed in some of the cell lines, similarly to what occurs with calcitriol treatment and other analogues [22]. In accordance with this hypothesis, we observed an increase in relative CYP24A1 mRNA in T98G cells treated with the analogue (100 nM; 24 h) (Supporting Information Figure S2) that could be a plausible explanation of the lack of effect on the reduction of cellular number in this glioma cell line. It has also been reported that splice variants of the enzyme may have implications for the antitumourigenic effects of the hormone and its analogues [23].

Effects of UVB1 analogue on cell migration

As known, the migratory capacity of tumour cells is an important ability acquired during tumour progression which allows them to metastasize. Therefore, a compound able to decrease cell migration could also be beneficial in cancer treatment. We evaluated the ability of the UVB1 analogue to reduce cell migration. To analyze this, we performed a 'wound healing' assay [24] in LM3, T98G, U251, HN12 and HN13 cell lines. As shown in Fig. 4, we found that the LM3 (Fig. 4A), T98G (Fig. 4B) and HN12 cells (Fig. 4C) displayed lower migratory rates upon treatment with UVB1 when compared with their respective controls. In contrast, the cell motility of U251 and HN13 cell lines was not affected by the presence of the analogue (data not shown).

Effects of UVB1 analogue on cell cycle

The 1α,25(OH)$_2$vitamin D$_3$ has been shown to promote cell cycle arrest in the G1/G0 phase in a variety of cell lines including leukemic cells [25], human pancreatic cancer cell line BxPC-3 [26] and human breast cancer cells [27, 28]. To understand the potential mechanism underlying the effects of UVB1 observed on cell viability, cell cycle analysis using flow cytometry of propidium iodide-stained cells was performed. As depicted in Fig. 5A, an arrest of HN13 cells in the G1/G0 phase was observed after treatment with 100 nM UVB1 (120 h). We found that UVB1 caused accumulation of cells in the G1/G0 phase of the cell cycle (63% of UVB1-treated vs. 53% of vehicle-treated cells; $^{***}p < 0.001$). These results are consistent with previous findings of the calcitriol effects on different squamous cell carcinoma cell lines [29–31].

To begin to understand the molecular mechanisms underlying UVB1 effects on cell viability, we analysed the expression of the proteins commonly involved in this process. As shown in Fig. 5B, UVB1 decreased cyclin D1 expression, a regulator of Cyclin Dependent Kinases (CDKs) and increased Bax, a marker of apoptosis, whereas it did not affect the expression of the CDK inhibitor p27 in HN13 cell line. VDR expression was not modulated by UVB1. In the U251 glioma cell line, UVB1 increased the expression of p27 and decreased cyclin D1, whereas it did not affect Bax expression. In this cell line, VDR expression was augmented with UVB1 treatment. All these preliminary results suggest that the UVB1 modulates the expression of a particular group of proteins, thus causing an antiproliferative effect specific to each cancer cell line and its context. It seems that the decrease of the expression of cyclin D1 protein is a common mechanism of action of UVB1 in both cell lines.

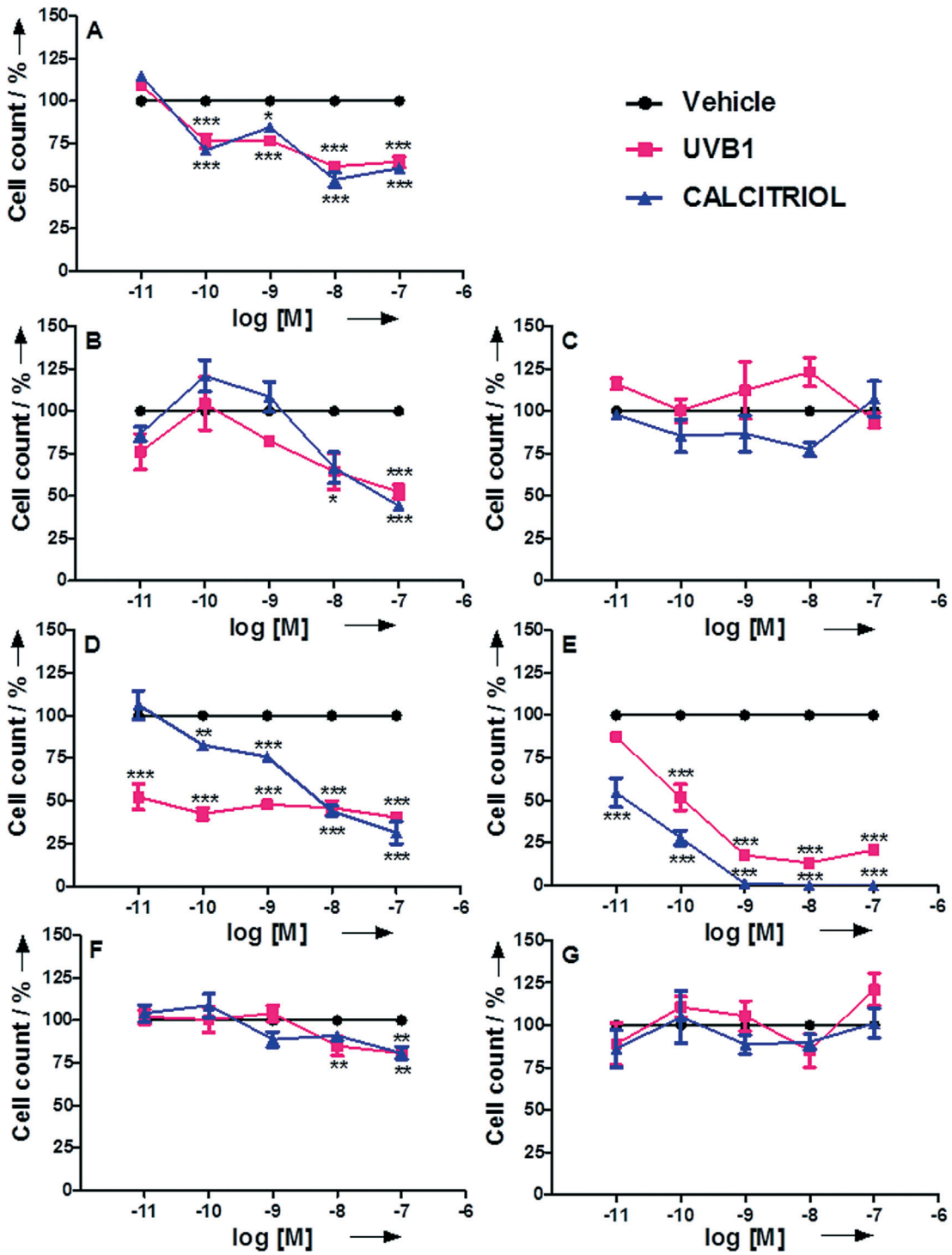

Figure 3. Dose-response effects of UVB1 analogue on cell count and its comparison with calcitriol. (A) Human colorectal carcinoma HCT116. (B) Human glioblastoma multiforme U251. (C) Human glioblastoma multiforme T98G. (D) Human head and neck squamous cell carcinoma HN13. (E) Human head and neck squamous cell carcinoma HN12. (F) Human mammary adenocarcinoma T47D. (G) Murine mammary adenocarcinoma LM3. Cells were exposed to the indicated doses of vehicle (isopropanol), UVB1 or calcitriol over a total period of 120 h. Cell count was expressed as percentage of the vehicle-treated cells. Data points represent means ± SD from four replicates; $^{*}p < 0.05$, $^{**}p < 0.01$ and $^{***}p < 0.001$ with respect to vehicle. The experiments were repeated three times for each cell line.

Table 1. IC_{50} of cell lines that responded to UVB1 and calcitriol treatments (nM)[a].

Cell line	UVB1	Calcitriol
HCT116	0.029	0.0074
U251	5.6	12.06
HN13	0.0016	1.98
HN12	0.071	0.084
T47D	5.7	0.54

[a] IC_{50}: half maximal inhibitory concentration.

Effects of UVB1 on blood calcium levels in animals

Vitamin D and many of its analogues induce hypercalcemia, a fact that limits the therapeutic efficacy of these compounds for cancer treatment. Therefore, analyses of the calcemic effects need to be performed for each novel analogue synthesised. Because of its significant antiproliferative activity and its important inhibition on cell migration in some cancer cell lines, UVB1 was then evaluated for its calcemic effects *in vivo*. Previous pharmacokinetic studies performed in normal mice indicated that calcitriol at 0.125 μg/mouse (approx. 5 μg/kg body weight) results in a $C_{max} > 10.0$ ng/mL and AUC >40.0 ng h/mL [32], exceeding the concentration needed for calcitriol anti-tumour activity *in vitro* [33]. Other studies using either calcitriol or vitamin D analogues at doses lower than 5 μg/kg body weight showed a reduction in tumour burden in animal models of cancer [31, 34, 35]. Therefore, in order to evaluate possible toxicological effects we began with the dose of 5 μg/kg body weight that has antitumour effects *in vivo* as a starting concentration for the studies of plasma calcium levels, with the idea of increasing the doses in escalating experiments. Mice were divided into three groups ($n = 5$/group) and given a daily intraperitoneal injection of calcitriol, UVB1 or vehicle at 5 μg/kg body weight for 4 days. Blood was collected prior to dose administration, then at 24, 48, 72 and 96 h post-treatment. The health condition of the animals was recorded. Plasma calcium levels were measured by reading the absorbance of metallochromic indicator Arsenazo III AA, as previously described [36]. Interestingly, UVB1 showed no hypercalcemic activity, although a tendency to increase plasma calcium levels within the normal range was observed when comparing with vehicle-treated animals (Fig. 6). Normal calcium levels range from 8.8 to 10.4 mg/dL [37]. Instead, calcitriol caused an increase in plasma calcium, as expected. We also observed the appearance of conjunctivitis, chills and thirst which are symptoms and signs that have been associated with hypercalcemia [38]. Moreover, mice that were treated with calcitriol died after 3 days of treatment, whereas mice treated with UVB1 remained alive and healthy during the entire examination period.

Additionally, an increase in haematocrit was observed (50 at 72 h; normal levels range from 39 to 47 [39] which is a sign of intoxication [40]). Visual observation of the internal organs of the animals treated with UVB1 such as liver, duodenum, lungs and kidneys showed no macroscopic morphological alterations.

As no hypercalcemia or other toxic signs were observed at the dose of 5 μg/kg body weight, and as UVB1 had marked antitumour effects on human cancer cell lines, we proposed to evaluate the effect of a higher UVB1 dose and for a prolonged period of time in N:NIH(S)-*Fox1*^{nu} mice, a widely used immunodeficient mouse model for performing human cell xenografts. Mice were divided into two groups ($n = 5$/group) and an injection of UVB1 or vehicle at 40 μg/kg body weight was given three times a week for a total period of 21 days. Blood was collected at the end of the period of treatment and the health condition of the animals was recorded. Plasma calcium levels were measured as previously described. As shown in Fig. 7, the treatment of N:NIH(S)-*Fox1*^{nu} mice with a 40 μg/kg body weight of the analogue produced neither hypercalcemia (Fig. 7A) nor kidney or liver histological alterations (Fig. 7B), which are important organs responsible for compound detoxification. In livers from mice treated with UVB1 and vehicle, no lobular or portal injuries were observed, and in kidneys, no glomerulopathies, vascular or interstitial lesions were evidenced. Furthermore, animals treated with this dose of UVB1 did not experiment a change in behaviour, weight loss or haematocrit alterations.

Discussion

In summary, we serendipitously synthesised a new Gemini analogue of 1α,25(OH)$_2$D$_3$ through a process based on a nickel-mediated conjugate addition of methyl acrylate to an alkynyl iodide derived from a new flexible and versatile synthetic method developed in our laboratories. Work is now in progress for the finding of a mechanistic rationale behind the formation of UVB1 side chain and the design of a stereoselective route leading to both C-20 epimers of UVB1. The biological evaluation indicated that this analogue exhibited high effectiveness in reducing cell count in two human head and neck squamous carcinoma (HN12 and HN13), one glioblastoma multiforme (U251), one colorectal carcinoma (HCT116) and one mammary adenocarcinoma (T47D) cell lines. Furthermore, in U251 and in HN13 cell lines, the reduction in cell number exerted by UVB1 was greater than that elicited by calcitriol. This reduction in cell counting was shown to occur through induction of cell cycle arrest, and this was accompanied by downregulation of cyclin D1 in HN13 and U251 cell lines. On the other hand, the lack of effect on the cell number in T98G cell line treated with calcitriol or UVB1 could be due to a high expression of the enzyme CYP24A1 mRNA, leading to degradation of calcitriol and the analogue.

In addition, an effect on cellular migration was demonstrated for one murine and two human cell lines. The inhibition in cell migration following UVB1 treatment observed in LM3 and T98G cell lines (that showed no effect in cell number) indicates that UVB1 also modulates other

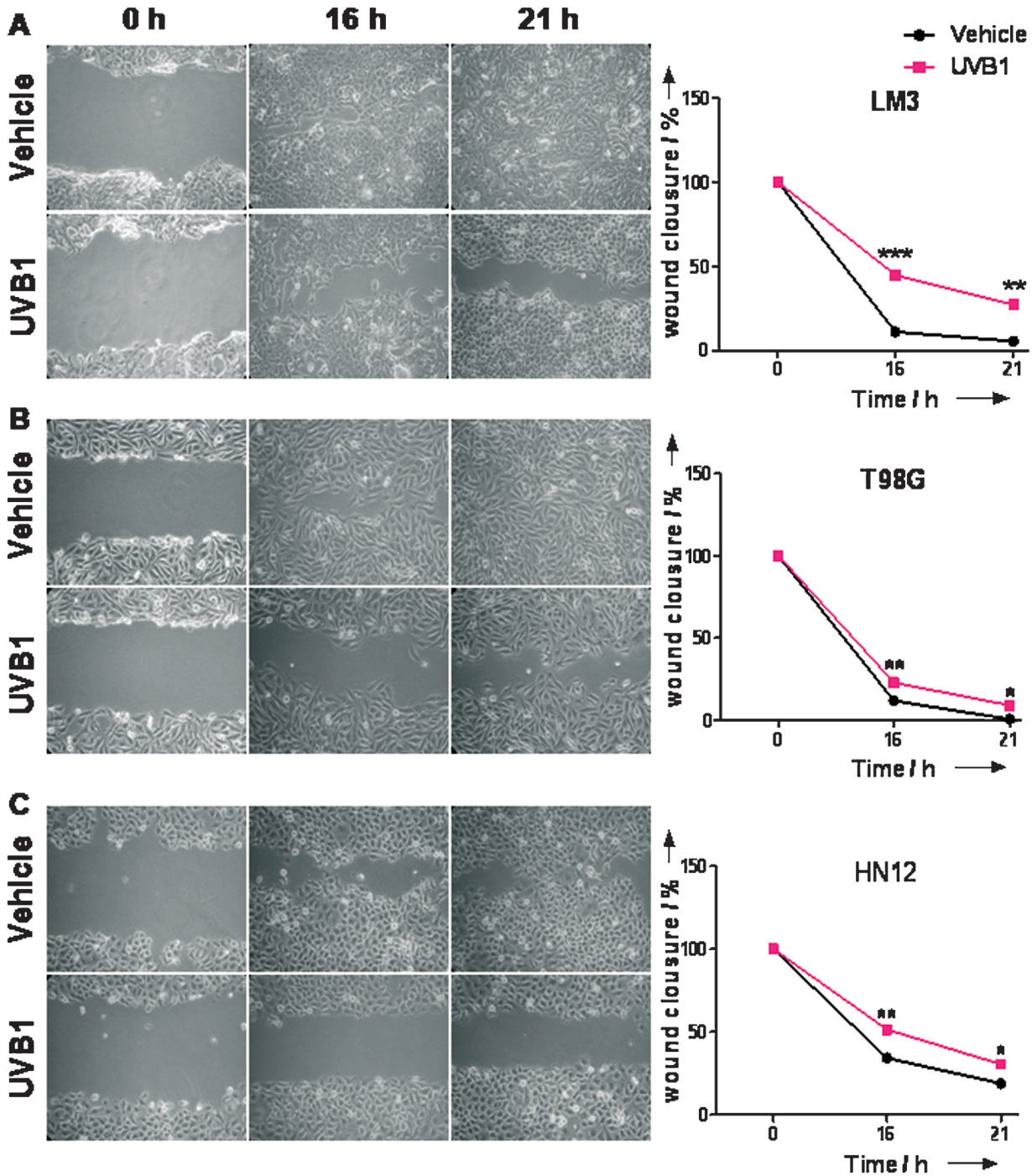

Figure 4. Wound healing assay of the (A) LM3, (B) T98G and (C) HN12 cell lines at 0, 16 and 21 h of culture. Cells were scratched by a 200 μL pipette tip [24]. The uncovered wound area was measured and quantified at different intervals with ImageJ 1.37 v. The experiment has been conducted three times. Two-way ANOVA and Bonferroni post test were applied. $^{*}p < 0.05$, $^{**}p < 0.01$ and $^{***}p < 0.001$.

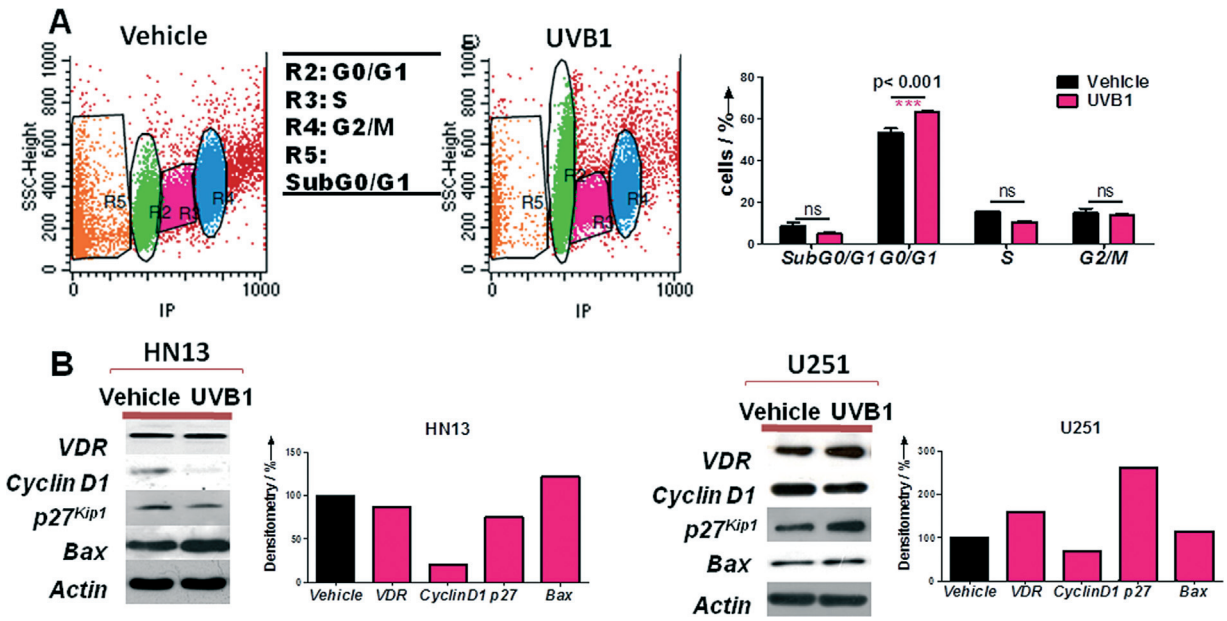

Figure 5. Flow cytometry analysis in HN13 cell line treated with UVB1 and Western blotting for VDR, Cyclin D1, p27 and Bax in HN13 and U251 cell line after treatment with the analogue. A) The cells were treated with UVB1 (100 nM; 120 h) and stained with PI in order to analyze the percentage of cells in the different phases of the cell cycle. B) Effect of UVB1 on VDR, Cyclin D1, p27 and Bax by Western blotting in HN13 and U251 cell line in response to the treatment with UVB1 (100 nM; 12 h). Actin was used as the loading control. The graphics of bars show the densitometry of bands.

important processes in the progression of cancer, such as cell motility.

Moreover, following animal treatment with UVB1, the serum calcium levels remained within the normal range and no toxicity on kidneys and livers was observed at the doses of 5 and 40 μg/kg. Altogether, these results suggest that this Gemini analogue exerts considerable antitumoural activity in cancer cell lines at non-hypercalcemic dosages and may have therapeutic potential for the treatment of different hyperproliferative disorders such as cancer.

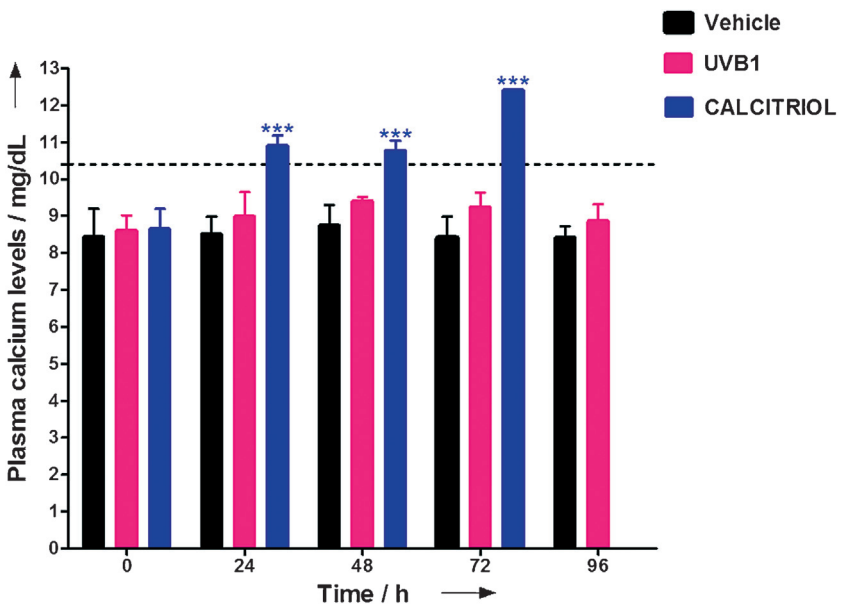

Figure 6. Plasma calcium levels in CF1 mice in response to daily intraperitoneal injections of vehicle (isopropanol), UVB1 or calcitriol during a period of 4 days. Animals were injected with 5 μg/kg body weight of compounds and plasma calcium was measured before the injection (0 h, basal levels) and at 24, 48, 72 and 96 h. Normal levels range from 8.8 to 10.4 mg/dL [37]. Values for calcitriol at 96 h were not available because animals died following 3 days of treatment due to hypercalcemia. Values are means ± SD from five animals in each group. The experiment was repeated two times. $^{***}p < 0.001$ with respect to vehicle.

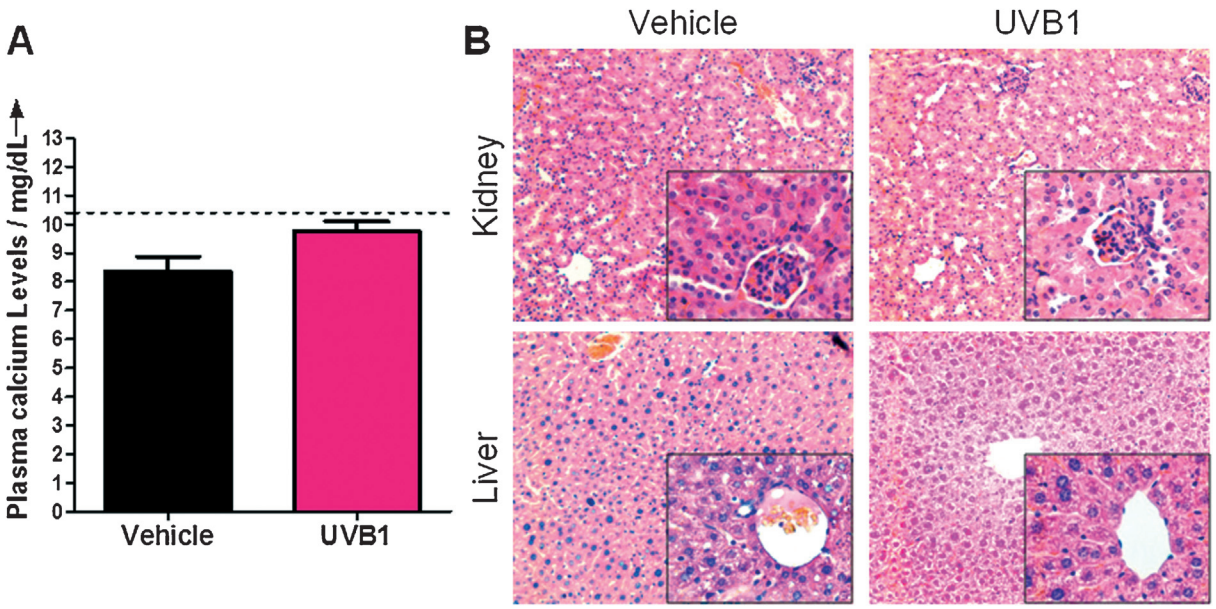

Figure 7. Plasma calcium levels in N:NIH(S)-*Fox1*^{nu} mice and histological examination of livers and kidneys from animals treated with UVB1 and vehicle. A) Plasma calcium levels in response to a three-times-a-week injection of vehicle (isopropanol) and UVB1 during a total period of 21 days. Animals were injected with 40 μg/kg body weight of compounds and plasma calcium was measured at the end of the period of treatment. Normal levels range from 8.8 to 10.4 mg/dL [37]. Values are means ± SD from five animals in each group. The experiment was repeated twice. B) Hematoxylin/eosin staining of livers and kidneys from animals treated with UVB1 and vehicle (isopropanol) at 40 μg/kg body weight. The sections of UVB1 and vehicle showed no histological damage. Magnification: ×100 and ×400 for the inset.

Experimental

Chemistry

General

Solvents were purified and dried by standard procedures. Flash chromatography was performed on silica gel (Merck 60, 230–400 mesh). Analytical TLC was performed on plates precoated with silica gel (Merck 60 F254, 0.25 mm). Melting points were obtained using a Gallenkamp apparatus and are uncorrected. Optical rotations were obtained using a Jasco P-2000 polarimeter. IR spectra were obtained using a Jasco FT/IR-6100 Type A spectrometer. ^{1}H NMR (400 MHz) and ^{13}C NMR (100 MHz) spectra were recorded on a Bruker ARX-400 spectrometer using TMS as the internal standard; chemical shifts (δ) are quoted in parts per million and coupling constants (J) in Hertz. Mass spectrometry (MS and HRMS) was carried out using a Hewlett-Packard 5988A spectrometer. Electrospray mass spectra (ESI-MS) were measured on a Bruker APEXQe FT-ICR MS.

*(3S)-Methyl 4-((tert-butyldimethylsilyl)oxy)-3-((3aR,4S,7aR)-4-((tert-butyldimethylsilyl)oxy)-7a-methyloctahydro-1H-inden-1-yl)butanoate (**3**)*

To a solution of compound **2** (6.9 g, 13.85 mmol) in EtOAc (165 mL) was added Pd/C (5%) (826 mg) and the resulting suspension was vigorously stirred at room temperature under H_2 atmosphere for 13 h. The mixture was then filtered through Celite and the filtrate concentrated under reduced pressure, affording compound **3** (6.8 g, 98%).

Compound **3**: colourless liquid, Rf: 0.71 (10% EtOAc/hexane); IR (NaCl, cm^{-1}): 2952.01, 2929.82, 2883.54, 2857.02, 1740.92, 1252.54, 1089.1; $[\alpha]^{24}_{D} = +20.41$ (c 2.43, $CHCl_3$); ^{1}H-NMR ($CDCl_3$, δ): 3.98 (1H, br s, H-8), 3.62 (3H, s, CH_3–OMe), 3.60 (1H, dd, $J = 9.9$, 3.3 Hz, H-21), 3.51 (1H, dd, $J = 9.9$, 5.6 Hz, H-21), 2.56 (1H, dd, $J = 15.8$, 3.6 Hz, H-22), 2.38 (1H, dd, $J = 15.8$, 9.1 Hz, H-22), 1.93 (1H, m), 1.79 (3H, m), 1.66 (1H, m), 1.55 (1H, m), 1.44–1.21 (6H, m), 1.12 (1H, m), 0.94 (3H, s, CH_3-18), 0.88 (9H, s, CH_3-*t*-Bu), 0.87 (9H, s, CH_3-*t*-Bu), −0.001 (9H, s, CH_3-Si), −0.01 (3H, s, CH_3-Si); ^{13}C-NMR ($CDCl_3$, δ): 173.8 (C=O), 69.2 (CH-8), 64.1 (CH_2-21), 52.7 (CH-17), 51.1 (CH_3–OMe), 50.5 (CH-14), 41.8 (C-13), 40.4 (CH_2), 39.2 (CH-20), 34.6 (CH_2), 34.3 (CH_2), 26.2 (CH_2), 25.9 (CH_3-^{t}Bu), 25.8 (CH_3-^{t}Bu), 22.8 (CH_2), 18.3 (C-*t*-Bu), 18.0 (C-*t*-Bu), 17.6 (CH_2), 14.1 (CH_3-18), −4.8 (CH_3-Si), −5.2 (CH_3-Si), −5.60 (CH_3-Si), 5.61 (CH_3-Si); MS (ESI) [*m/z*, (%)]: 499 (M^{+}+1, 100), 358 (25); HRMS (ESI): 499.6590 calculated for $C_{27}H_{55}O_4Si_2$, found 499.6588.

*(3S)-4-((tert-Butyldimethylsilyl)oxy)-3-((3aR,4S,7aR)-4-((tert-butyldimethylsilyl)oxy)-7a-methyloctahydro-1H-inden-1-yl)-butan-1-ol (**4**) and (3S)-4-((tert-butyldimethylsilyl)oxy)-3-((3aR,4S,7aR)-4-((tert-butyldimethylsilyl)oxy)-7a-methyloctahydro-1H-inden-1-yl)butanal (**5**)*

To a solution of ester **3** (650 mg, 1.31 mmol) in hexane (50 mL) at −78°C Dibal was added (2.62 mL, 2.62 mmol and 1 M

solution in hexane) and the mixture was stirred at this temperature for 30 min, before adding *t*-BuOMe (7.91 mL) and H_2O (0.98 mL). The cooling bath was removed and vigorous stirring was continued till the formation of a white gel. H_2O (0.98 mL) and a 4 M aqueous solution of NaOH (0.98 mL) were added and stirring was continued till the formation of a white solid. Na_2SO_4 and silica gel were added and the mixture was stirred for 30 min. Filtration of the solids and evaporation of the filtrate gave a residue which was chromatographed on silica gel using 5% EtOAc/hexane as eluent, affording compounds **4** (450 mg, 73%) and **5** (125 mg, 20%).

Compound **4**: colourless liquid, Rf: 0.37 (10% EtOAc/hexane); IR (NaCl, cm^{-1}): 3361.81, 2953.45, 2929.34, 2883.54, 2857.02, 1253.02, 835.50; $[\alpha]^{23}_D = +24.56$ (c 1.32, $CHCl_3$); ^{1}H-NMR ($CDCl_3$, δ): 4.00 (1H, br s, CH-8), 3.70 (2H, dd, $J = 10.0$, 1.9 Hz, H-21, OH), 3.61 (1H, m, H-23), 3.45 (1H, dd, $J = 10.0$, 6.6 Hz, H-21), 3.21 (1H, t, $J = 5.4$ Hz, H-23), 1.89 (2H, m), 1.76 (2H, m), 1.70–1.49 (4H, m), 1.40–1.20 (6H, m), 1.13 (1H, m), 0.94 (3H, s, CH_3-18), 0.90 (9H, s, CH_3-*t*-Bu), 0.88 (9H, s, CH_3-*t*-Bu), 0.07 (6H, s, CH_3-Si), 0.01 (3H, s, CH_3–Si), 0.001 (3H, s, CH_3–Si); ^{13}C-NMR ($CDCl_3$, δ): 69.3 (CH-8), 66.1 (CH_2-21), 60.8 (CH_2-23), 52.8 (CH-14), 51.1 (CH-17), 42.1 (C-13), 41.3 (CH-20), 40.6 (CH_2), 34.9 (CH_2), 34.3 (CH_2), 26.8 (CH_2), 25.8 (CH_3-^{t}Bu), 25.8 (CH_3-*t*-Bu), 22.9 (CH_2), 18.2 (C-*t*-Bu), 17.9 (C-*t*-Bu), 17.6 (CH_2), 13.9 (CH_3-18), −4.8 (CH_3–Si), −5.2 (CH_3–Si), −5.4 (CH_3–Si), −5.5 (CH_3–Si); MS (ESI) [*m/z*, (%)]: 471 (M^++1, 100), 472 (M^++2, 25); HRMS (ESI): 471.3684 calculated for $C_{26}H_{55}O_3Si_2$, found 471.3674.

Compound **5**: colourless liquid, Rf: 0.71 (10% EtOAc/hexane); IR (NaCl, cm^{-1}): 2952.97, 2929.82, 2883.54, 2857.02, 1726.94, 1471.94, 853.50; $[\alpha]^{22}_D = +23.60$ (c 1.72, $CHCl_3$); ^{1}H-NMR ($CDCl_3$, δ): 9.73 (1H, d, $J = 3.4$ Hz, C**H**O), 3.99 (1H, br s, CH-8), 3.67 (1H, dd, $J = 9.6$, 3.7 Hz, H-21), 3.40 (1H, dd, $J = 9.6$, 7.3 Hz, H-21), 2.57 (1H, m, H-22), 2.38 (1H, ddd, $J = 16.4$, 9.0, 3.4 Hz, H-22), 2.09 (1H, m), 1.37–1.53 (5H, m), 1.43–1.20 (6H, m), 1.13 (1H, t, $J = 12.5$ Hz), 0.95 (3H, s, CH_3-18), 0.87 (9H, s, CH_3-*t*-Bu), 0.85 (9H, s, CH_3-*t*-Bu), 0.011 (3H, s, CH_3–Si), −0.001 (6H, s, CH_3–Si), 0.014 (3H, s, CH_3–Si); ^{13}C-NMR ($CDCl_3$, δ): 202.8 (C=O), 69.1 (CH-8), 65.6 (CH_2-21), 52.7 (CH-14), 50.8 (CH-17), 45.9 (CH_2), 42.1 (C-13), 40.6 (CH_2), 39.1 (CH-20), 34.2 (CH_2), 26.6 (CH_2), 25.8 (CH_3-*t*-Bu), 25.8 (CH_3-*t*-Bu), 22.9 (CH_2), 18.2 (C-*t*-Bu), 17.9 (C-*t*-Bu), 17.5 (CH_2), 14.2 (CH_3-18), −4.8 (CH_3–Si), −5.2 (CH_3−Si), −5.6 (CH_3–Si), −5.6 (CH_3–Si); MS (ESI) [*m/z*, (%)]: 467 (M^+−1, 100); HRMS (ESI): 467.3367 calculated for $C_{26}H_{51}O_3Si_2$, found 467.3366.

*Oxidation of alcohol **4** to aldehyde **5***

To a solution of alcohol **4** (780 mg, 1.66 mmol) in CH_2Cl_2 (15 mL) were added 4 Å molecular sieves (500 mg), *N*-methylmorpholine *N*-oxide (NMO) (583 mg, 4.98 mmol) and catalytic amount of tetrapropylammonium perruthenate (TPAP). The greenish resulting suspension was stirred at room temperature for 2 h. After solvent evaporation the residue was chromatographed on silica gel using 5% EtOAc/hexane as eluent, affording aldehyde **5** (705 mg, 90%) the spectral data of which were similar to those obtained previously.

*tert-Butyl(((2S)-2-((3aR,4S,7aR)-4-((tert-butyldimethylsilyl)-oxy)-7a-methyloctahydro-1H-inden-1-yl)pent-4-yn-1-yl)-oxy)dimethylsilane (**7**)*

To a solution of aldehyde **5** (194 mg, 0.41 mmol) in MeOH (20 mL) was added **6** (432 mg, 2.1 mmol). The mixture was cooled to 0°C and K_2CO_3 (287 mg, 2.1 mmol) was added. Stirring was continued for 4 h, after adding H_2O (30 mL) the aqueous phase was extracted with EtOAc (3 × 20 mL) and the combined organic phases were dried, filtered and concentrated under vacuum. The residue was chromatographed on silica gel using 0.2% EtOAc/hexane as eluent, affording alkyne **7** (118 mg, 61%).

Compound **7**: white solid, mp: 70°C, Rf: 0.78 (10% EtOAc/hexane); IR (NaCl, cm^{-1}): 3313.11, 2952.28, 2930.31, 2896.56, 2882.09, 2857.09, 2117.47, 1253.51; $[\alpha]^{25}_D = +29.23$ (c 2.4, $CHCl_3$); ^{1}H-NMR ($CDCl_3$, δ): 4.01 (1H, br s, H-8), 3.70 (1H, dd, $J = 9.7$, 3.3 Hz, H-21), 3.50 (1H, dd, $J = 9.7$, 7.8 Hz, H-21), 2.57 (1H, m, H-22), 2.28 (1H, ddd, $J = 16.7$, 6.2, 2.5 Hz, H-22), 1.90 (1H, t, $J = 2.5$ Hz, H-24), 1.87 (1H, m), 1.83–1.49 (5H, m), 1.46–1.22 (7H, m), 0.92 (3H, s, CH_3-18), 0.89 (9H, s, CH_3-^{t}Bu), 0.88 (9H, s, CH_3-^{t}Bu), 0.05 (6H, s, CH_3–Si), 0.01 (3H, s, CH_3–Si), −0.01 (3H, s, CH_3–Si); ^{13}C-NMR ($CDCl_3$, δ): 83.2 (C-23), 69.4 (CH-24), 69.3 (CH-8), 63.2 (CH_2-21), 52.7 (CH-14), 49.5 (CH-17), 42.0 (C-13), 41.4 (CH-20), 40.2 (CH_2), 34.4 (CH_2), 26.3 (CH_2), 26.0 (CH_3-*t*-Bu), 25.8 (CH_3-*t*-Bu), 23.0 (CH_2), 18.7 (CH_2), 18.3 (C-*t*-Bu), 18.0 (C-*t*-Bu), 17.7 (CH_2), 14.1 (CH_3-18), −4.8 (CH_3–Si), −5.2 (CH_3–Si), −5.4 (CH_3–Si), −5.4 (CH_3–Si); MS (FAB^+) [*m/z*, (%)]: 465 (M^++1, 75), 385.2 (20), 299.1 (100), 245.1 (70); HRMS (FAB^+): 465.3579 calculated for $C_{27}H_{53}O_2Si_2$, found 465.3576.

*(2S)-2-((3aR,4S,7aR)-4-((tert-Butyldimethylsilyl)oxy)-7a-methyloctahydro-1H-inden-1-yl)pent-4-yn-1-ol (**8**)*

To a solution of alkyne **7** (118 mg, 0.25 mmol) in THF (5 mL) was added tetrabutylammonium fluoride (TBAF) (1 M solution in THF, 1 mL, 1 mmol) and the mixture was stirred at room temperature for 2 h. Saturated aqueous solution of NH_4Cl (10 mL) was added and the product was extracted with EtOAc (3 × 10 mL). The combined organic phases were dried on Na_2SO_4, filtered and concentrated under vacuum, affording a residue which was chromatographed on silica gel using 5% EtOAc/hexane as eluent, affording alcohol **8** (89 mg, 99%).

Compound **8**: colourless liquid, Rf: 0.17 (10% EtOAc/hexane); IR (NaCl, cm^{-1}): 3401.12, 3311.18, 2930.31, 2900.41, 2857.02, 2117.69, 1375.96, 1020.16; $[\alpha]^{22}_D = +30.58$ (c 1.78, $CHCl_3$); ^{1}H-NMR ($CDCl_3$, δ): 4.00 (1H, br s, H-8), 3.82 (1H, dd, $J = 10.9$, 3.1 Hz, H-21), 3.61 (1H, dd, $J = 10.9$, 7.0 Hz, H-21), 2.56 (1H, m, H-22), 2.34 (1H, ddd, $J = 17.0$, 6.6, 2.6 Hz, H-22), 1.98 (1H, t, $J = 2.6$ Hz, H-24), 1.90–1.59 (5H, m), 1.58–1.21 (8H, m), 0.92 (3H, s, CH_3-18), 0.88 (9H, s, CH_3-*t*-Bu), 0.00 (3H, s, CH_3–Si), −0.01 (3H, s, CH_3–Si); ^{13}C-NMR ($CDCl_3$, δ): 82.9 (C-23), 70.2 (CH-24), 69.2 (CH-8), 64.2 (CH_2-21), 52.7 (CH-14), 49.5 (CH-17), 41.9 (C-13), 40.9 (CH-20), 40.1 (CH_2), 34.3 (CH_2), 26.4 (CH_2), 25.8 (CH_3-*t*-Bu), 22.9 (CH_2), 19.3 (CH_2), 17.9 (C-*t*-Bu), 17.6 (CH_2), 13.9 (CH_3-18), −4.8 (CH_3–Si), −5.2 (CH_3–Si); MS (FAB^+) [*m/z*, (%)]: 351 (M^++1, 100); HRMS (FAB): 351.2714 calculated for $C_{21}H_{39}O_2Si$, found 351.2713.

*tert-Butyl(((3aR,4S,7aR)-1-((S)-1-iodopent-4-yn-2-yl)-7a-methyloctahydro-1H-inden-4-yl)oxy)dimethylsilane (**9**)*
To a solution of alcohol **8** (83 mg, 0.24 mmol) in THF (4 mL) were sequentially added PPh_3 (74 mg, 0.28 mmol) and imidazole (48 mg, 0.71 mmol). The mixture was cooled to 0°C and I_2 (66 mg, 0.26 mmol) was added. After the addition, the cooling bath was removed and the mixture stirred at room temperature for 1 h. An aqueous saturated solution of $NaHCO_3$ (10 mL) was added and the product extracted with EtOAc (3 × 15 mL). The combined organic phases were washed with a 10% aqueous solution of $Na_2S_2O_3$ (50 mL) and brine (50 mL) dried and concentrated under vacuum, affording a residue which was chromatographed on silica gel using 5% EtOAc/hexane as eluent, affording iodide **9** (109 mg, 77%).

Compound **9**: colourless liquid, Rf: 0.7 (10% EtOAc/hexane); IR (NaCl, cm^{-1}): 3311.18, 2949.59, 2930.31, 2878.24, 2856.06, 2117.46, 1251.58; $[\alpha]^{23}_D = +27.54$ (c 4.45, $CHCl_3$); ^{1}H-NMR ($CDCl_3$, δ): 4.00 (1H, s ancho, H-8), 3.67 (1H, dd, *J* = 9.7, 1.9 Hz, H-21), 3.27 (1H, dd, *J* = 9.7, 5.6 Hz, H-21), 2.62 (1H, m, H-22), 2.23 (1H, ddd, *J* = 17.0, 7.3, 2.6 Hz, H-22), 1.99 (1H, t, *J* = 2.6 Hz, H-24), 1.88–1.55 (5H, m), 1.45–1.18 (8H, m), 0.96 (3H, s, CH_3-18), 0.88 (9H, s, CH_3-^{t}Bu), 0.01 (3H, s, CH_3–Si), −0.01 (3H, s, CH_3–Si); ^{13}C-NMR ($CDCl_3$, δ): 81.6 (C-23), 70.3 (CH-24), 69.2 (CH-8), 53.1 (CH-17), 52.6 (CH-14), 42.1 (C-13), 40.21 (CH-20), 40.20 (CH_2), 34.2 (CH_2), 26.5 (CH_2), 25.8 (CH_3-^{t}Bu), 22.7 (CH_2), 17.9 (C-^{t}Bu), 17.5 (CH_2), 15.8 (CH_2), 14.6 (CH_3-18), –4.8 (CH_3–Si), –5.1 (CH_3–Si); MS (FAB^+) [*m/z*, (%)]: 461 (M^++1, 20), 370 (35), 329 (65), 290 (71); HRMS (FAB): 461.1731 calculated for $C_{21}H_{38}IOSi$, found 461.1730.

*(6S)-Dimethyl-6-((3aR,4S,7aR)-4-((tert-butyldimethylsilyl)-oxy)-7a-methyloctahydro-1H-inden-1-yl)-4-methylenedecanedioate (**10**) and (5S)-methyl-5-((3aR,4S,7aR)-4-((tert-butyldimethylsilyl)oxy)-7a-methyloctahydro-1H-inden-1-yl)oct-7-ynoate (**11**)*
A flame-dried 50 mL flask was charged with activated Zn powder (165 mg, 2.5 mmol), anhydrous pyridine (4 mL), $NiCl_2 \cdot 6H_2O$ (119 mg, 0.5 mmol) and methyl acrylate (1.3 mL, 12 mmol) and the mixture was warmed to 65°C until the blue colour turned to a reddish brown solution. The mixture was cooled to 0°C and a solution of iodide **9** (78 mg, 0.17 mmol) in pyridine (3 mL) added. Stirring was continued for 90 min allowing the mixture to reach room temperature. The reaction mixture was poured into 15 mL of EtOAc and the resulting precipitate was filtered through a pad of Celite and the filtrate was washed with 10% aqueous solution of $CuSO_4$ (3 × 15 mL), H_2O (2 × 15 mL) and brine (15 mL). Drying (Na_2SO_4) and solvent evaporation gave a residue which was chromatographed on silica gel using 15% EtOAc/hexane as eluent, affording ester **11** (30 mg, 42%) together with unexpected diester **10** (35 mg, 40%).

Compound **10**: colourless liquid; Rf: 0.36 (10% EtOAc/hexane); ^{1}H-NMR ($CDCl_3$, δ): 4.70 (2H, br s), 4.0 (1H, br s, CH-8), 3.20 (3H, s, MeO), 3.50 (3H, s, MeO), 2.60–2.20 (8H, m), 1.90–1.00 (17H, m), 0.90 (3H, s, CH_3-18), 0.85 (9H, s, CH_3-*t*-Bu), −0.02 (6H, s, CH_3–Si); ^{13}C-NMR ($CDCl_3$, δ): 174.6 (C=O), 174.0 (C=O), 147.2 (C), 111.2 (=CH_2), 69.7 (CH-8), 53.3 (CH), 53.2 (CH), 51.9 (CH_3), 51.7 (CH_3), 41.1 (CH_2), 39.6 (CH_2), 36.4 (CH), 35.4 (CH_2), 34.8 (CH_2), 32.8 (CH_2), 30.4 (CH_2), 30.0 (CH_2), 26.4 (CH_2), 26.2 (C-*t*-Bu), 23.3 (CH_2), 19.8 (CH_2), 18.0 (CH_2), 14.5 (CH_3-18), −4.4 (CH_3-Si), −4.8 (CH_3–Si); HRMS (ESI): 509.36568 calculated for $C_{29}H_{53}O_5Si$, found 509.36551.

Compound **11**: colourless liquid; Rf: 0.62 (10% EtOAc/hexane); IR (NaCl, cm^{-1}): 3312.98, 2949.55, 2930.93, 2878.35, 2857.23, 2117.49, 1741.62; $[\alpha]^{25}_D = +17.84$ (c 1, $CHCl_3$); ^{1}H-NMR ($CDCl_3$, δ): 3.99 (1H, br s, H-8), 3.66 (3H, s, OC**H**$_3$), 2.31 (2H, m, 2H-24), 1.91 (1H, t, *J* = 2.5 Hz, H-2′), 1.87–1.22 (19H, m), 0.89 (3H, s, CH_3-18), 0.88 (9H, s, CH_3-*t*-Bu), 0.003 (3H, s, CH_3–Si), −0.001 (3H, s, CH_3–Si); ^{13}C-NMR ($CDCl_3$, δ): 174.1 (C=O), 82.7 (C-1′), 69.7 (CH-2′), 69.4 (CH-8), 52.9 (CH-17), 52.5 (CH-14), 51.4 (O**C**H$_3$), 41.9 (C-13), 40.2 (CH_2), 37.9 (CH-20), 34.4 (CH_2), 34.3 (CH_2), 30.9 (CH_2), 26.8 (CH_2), 25.8 (CH_3-*t*-Bu), 22.9 (CH_2), 21.6 (CH_2), 20.6 (CH_2), 18.0 (C-*t*-Bu), 17.7 (CH_2), 13.8 (CH_3-18), −4.8 (CH_3–Si), −5.2 (CH_3–Si); MS (FAB^+) [*m/z*, (%)]: 443 (M^++Na, 100), 396 (29); HRMS (FAB): 443.2952 calculated for $C_{28}H_{44}O_3SiNa$, found 443.2958.

*(7S)-7-((3aR,4S,7aR)-4-((tert-Butyldimethylsilyl)oxy)-7a-methyloctahydro-1H-inden-1-yl)-2,11-dimethyl-5-methylenedodecane-2,11-diol (**12**)*
Diester (**10**) (130 mg, 0.25 mmol) in dry THF (10 mL) was cooled to −78°C. MeLi (1 mL 1.5 mmol of a 1.5 M in ether) was added dropwise and the mixture stirred at −78°C for 1 h. Aqueous 5% solution of HCl was added and the product extracted with *t*-BuOMe. The organic phases were dried and concentrated to give a residue which was chromatographed on silica gel using 30% EtOAc/hexane as eluent, affording diol **12** in almost quantitative yield.

Compound **12**: colourless liquid; Rf: 0.37 (50% EtOAc/hexane); ^{1}H-NMR ($CDCl_3$, δ): 4.70 (1H, br s, =CH_2), 4.60 (1H, br s, =CH_2), (3.96 (1H, br s, CH-8), 2.25–1.10 (25H, m), 1.25 (3H, s, CH_3), 1.20 (3H, s, CH_3), 0.90 (3H, s, CH_3-18), 0.85 (9H, s, CH_3-*t*-Bu), −0.03 (6H, s, CH_3–Si); ^{13}C-NMR ($CDCl_3$, δ): 149.2 (C), 110.2 (=CH_2), 70.9 (C), 70.8 (C), 69.4 (CH-8), 53.0 (CH), 52.9 (CH), 44.6 (CH_2), 42.0 (CH_2), 40.0 (CH_2), 38.0 (CH_2), 36.3 (CH), 34.4 (CH_2), 30.8 (CH_2), 29.9 (CH_2), 29.4 (CH_3), 29.3 (CH_3), 29.2 (CH_3), 28.9 (CH_3), 25.9 (CH_2), 25.8 (CH_3-*t*-Bu), 22.9 (CH_2), 18.5 (CH_2), 17.9 (CH_2), 17.6 (C-*t*-Bu), 14.1 (CH_3-18), −4.8 (CH_3–Si), −5.2 (CH_3–Si); HRMS (ESI): 509.43845 calculated for $C_{31}H_{61}O_3Si$, found 509.43828.

*(9S)-9-((3aR,4S,7aR)-4-((tert-Butyldimethylsilyl)oxy)-7a-methyloctahydro-1H-inden-1-yl)-2,2,4,4,13,13,15,15-octamethyl-7-methylene-3,14-dioxa-2,15-disilahexadecane (**13**)*
To a solution of compound **12** (130 mg, 0.24 mmol) in CH_3CN (20 mL) were added a few drops of 40% aqueous HF solution and the mixture was stirred at room temperature for 2 h. Saturated aqueous solution of $NaHCO_3$ (5 mL) was added and the product was extracted with *t*-BuOMe (3 × 10 mL). The combined organic phases were dried over Na_2SO_4 and concentrated affording the expected triol which was used in

the next reaction without further purification. To a solution of the above prepared triol in dry CH_2Cl_2 (20 mL) was added pyridinium dichromate (PDC) (256 mg, 0.68 mmol) and the mixture stirred overnight at room temperature. It was then filtered through a pad of Celite and the filtrate concentrated to afford the expected ketone which was used in the next reaction without further purification. To a solution of the above prepared ketone in dry THF (20 mL) was added 1-(trimethylsilyl)imidazole (TMS-imidazole) (660 μL, 4.4 mmol) and the mixture stirred overnight at room temperature. Solvent evaporation gave a residue which was chromatographed on silica gel using 8% EtOAc/hexane as eluent, affording ketone **13** (88 mg, 64% from diol **12**, 3 steps).

Compound **13**: colourless liquid; Rf: 0.83 (90% EtOAc/hexane); ^{1}H-NMR ($CDCl_3$, δ): 4.70 (1H, br s, $=CH_2$), 4.60 (1H, br s, $=CH_2$), 2.45 (1H, dd, $J = 11.4, 7.6$ Hz, H-14), 2.20–1.22 (24H, m), 1.20 (6H, s, CH_3), 1.15 (6H, s, CH_3), 0.62 (3H, s, CH_3-18), 0.05 (18H, s, CH_3–Si); ^{13}C-NMR ($CDCl_3$, δ): 211.9 (C=O), 148.8 (C), 110.4 ($=CH_2$), 73.9 (C), 73.6 (C), 61.7 (CH), 53.0 (CH), 49.8 (C), 45.4 (CH_2), 43.0 (CH_2), 40.9 (CH_2), 39.8 (CH_2), 38.7 (CH_2), 36.2 (CH), 30.9 (CH_2), 29.9 (CH_3), 29.8 (CH_3), 29.7 (CH_3), 25.6 (CH_2), 23.9 (CH_2), 19.0 (CH_2), 18.9 (CH_2), 12.8 (CH_3-18), 2.6 (CH_3–Si), 2.6 (CH_3–Si).

(1R,3S,Z)-5-((E)-2-((1R,3aS,7aR)-1-((S)-2,11-Dihydroxy-2,11-dimethyl-8-methylenedodecan-6-yl)-7a-methylhexahydro-1H-inden-4(2H)-ylidene)ethylidene)-4-methylenecyclohexane-1,3-diol (UVB1)

To a solution of phosphine oxide **14** (292 mg, 0.492 mmol) in dry THF (10 mL) at −78°C was added dropwise *n*-BuLi (0.177 mL of a 2.5 M solution in hexane) and the resulting red solution was stirred at the same temperature for 1 h in the dark, before adding via cannula a solution of ketone **13** (88 mg, 0.164 mmol) in THF (5 mL). The mixture was stirred for 2 h then quenched with NH_4Cl (a few drops) and extracted with EtOAc (2 × 10 mL). The combined organic phases were washed with an aqueous saturated solution of $NaHCO_3$. After solvent evaporation, the residue was purified by flash column chromatography (100% hexane → 10% EtOAc/hexane) to afford the protected analogue which was dissolved in THF (5 mL) before adding TBAF (1.2 mL, 1.0 M, 1.2 mmol) at room temperature. The mixture was stirred for 24 h at room temperature, quenched with NH_4Cl (1 mL) and extracted with EtOAc (2 × 10 mL). The combined organic phases were washed with an aqueous saturated solution of NH_4Cl. After drying (Na_2SO_4) and solvent evaporation, the residue was purified by flash column chromatography (100% hexane → 95% EtOAc/hexane) to afford UVB1 (60 mg, 70% from ketone **13**, 2 steps).

UVB1: brown solid; mp: 82.6°C; Rf: 0.40 (EtOAc); $[\alpha]^{23}_D = -2.76$ (c 0.15, $CHCl_3$); ^{1}H-NMR ($CDCl_3$, δ): 6.25 (1H, d, $J = 11.2$ Hz, H-6), 6.01 (1H, d, $J = 11.2$ Hz, H-7), 5.25 (1H, br s, H-19), 4.90 (1H, br s, H-19), 4.70 (1H, br s, $=CH_2$), 4.60 (1H, br s, $=CH_2$), 4.35 (1H, dd, $J = 7.8, 4.2$ Hz, H-1), 4.11 (1H, m, H-3), 2.75 (1H, m), 2.50 (1H, m), 2.30 (2H, m), 1.15 (6H, s), 1.10 (6H, s), 0.50 (3H, s, CH_3-18); ^{13}C-NMR ($CDCl_3$, δ): 149.0 (C), 147.7 (C), 142.6 (C), 133.2 (C), 124.7 (CH), 117.1 (CH), 111.6 ($=CH_2$), 110.4 ($=CH_2$), 71.0 (CH), 70.8 (C), 70.5 (C), 66.6 (CH), 56.1 (CH), 52.8 (CH), 45.7 (C), 45.1 (CH_2), 44.5 (CH_2), 42.8 (CH_2), 41.8 (CH_2), 40.2 (CH_2), 39.5 (CH_2), 37.0 (CH), 30.9 (CH_2), 29.9 (CH_2), 29.4 (CH_2), 29.3 (CH_3), 29.2 (CH_3), 29.0 (CH_3), 28.9 (CH_3), 25.9 (CH_2), 22.1 (CH_2), 18.7 (CH_2), 12.3 (CH_3); HRMS (ESI): 529.42514 calculated for $C_{34}H_{57}O_4$, found 529.42557.

In vitro and *in vivo* biological evaluation

Chemicals and reagents

1α,25-Dihyroxyvitamin D_3 (calcitriol) and UVB1 were reconstituted in 100% HPLC-grade isopropanol and stored protected from light at −20°C. The amount of 1α,25$(OH)_2D_3$ and its analogue was determined by UV spectrophotometry between 200 and 300 nm. Both drugs were dissolved in isopropanol to the concentration of 10^{-3} M and subsequently diluted in the culture medium to reach the required concentrations (ranging from 0.01 to 100 nM).

Cell lines

Biological evaluation of UVB1 was performed in seven different cancer cell lines. The human cell lines used were as follows: human glioblastoma T98G and U251, head and neck squamous cell carcinoma HN12 and HN13, colorectal carcinoma HCT116 and mammary adenocarcinoma T47D. We also employed the murine mammary adenocarcinoma LM3 cell line which was kindly donated by the Instituto de Oncología A Roffo. All the cell lines were maintained at 37°C, 5% CO_2 in DMEM supplemented with 100 U/mL penicillin, 100 U/mL streptomycin, 4 mM glutamine and 10% fetal calf serum (FCS) except for the LM3 that was 5% FCS.

Cell count and viability assay

The cell lines were plated at a density of 500–2500 cells/well into 96 multi-well plates in complete medium, and treated with 0.01–100 nM of calcitriol, UVB1 or vehicle (isopropanol), which resulted in a maximum of 0.1% v/v alcohol in the assay wells. We did not find that this amount of alcohol (or lower concentrations) had any significant effect on the cell lines (medium was changed every 2 days). For the dose–response experiments, the cells were incubated for a maximum of 120 h. They were then washed with PBS 1×, trypsinised and resuspended in complete medium (100 μL) and counted manually using a hemocytometer. Additionally, cellular viability was assessed by the WST-1 colorimetric assay (Roche, Argentina). Following analogue treatment the cells were incubated for 1 h with the tetrazolium salt WST-1 (4-[3-(4-iodophenyl)-2-(4-nitrophenyl)-2*H*-5-tetrazolio]-1,3-benzene-disulfonate) and the formazan product determined by absorbance reading at 440 nm. The reference wavelength was 690 nm.

Quantitative reverse transcription-polymerase chain reaction (qRT-PCR)

Total RNA was isolated from 4×10^5 T98G treated cells (vehicle, UVB1 and calcitriol during 24 h) using an SV Total

RNA Isolation System following the manufacturer's instructions. mRNA was converted into cDNA using the Moloney murine leukemia virus reverse transcriptase (MLV-RT; Promega). Quantitative RT-PCR analysis was carried out by using GAPDH mRNA amplification as an internal standard. RT-PCR products were analysed by electrophoresis on a 1.5% agarose gel stained with ethidium bromide. Relative quantification of mRNA by qPCR was performed using a Rotor-Gene 6000 (Corbett Research). Forward and reverse primers for the reaction were as follows: 5′-GCTTTACCCAAAGGAATTGTCCGC-3′ (forward) and 5′-TCCCAGCACTCAGTCCGCTT-3′ (reverse) for CYP24A1; 5′-TTCACCACCATGGAGAAGGC-3′ (forward) and 5′-AGTGATGGCATGGACTGTGGTC-3′ (reverse) for GAPDH. RT-PCR results were analysed using the $2^{-\Delta\Delta CT}$ method [41]. The expression of the gene of interest is presented relative to an internal control gene. The advantage of the comparative CT method is the ability to present the data as 'fold change' in expression. The CT values of target mRNA were normalised with the CT value of the housekeeping gene GAPDH using the formula $\Delta CT = CT\ (CYP24A1) - CT\ (GAPDH)$ and the data are presented as $2^{-\Delta CT}$. The method was further used to determine the relative expression of the same gene from three samples: $\Delta\Delta CT = CT$ (sample UVB1/calcitriol) $-$ CT (sample control). The data are presented as $2^{-\Delta\Delta CT}$.

Wound-healing assay

The LM3, T98G, U251, HN12 and HN13 cancer cells were seeded onto sterile 3.5 mm plates and allowed to recover for a confluent cell monolayer. A straight scratch was made using a 200 μL plastic pipette tip [24]. The plates were rinsed with PBS to remove floating cells and then fresh medium containing the analogue and vehicle 100 nM was added to each plate. The photos were taken at 0, 16 and 21 h after scratching. Images were recorded with an inverted phase microscope NIKON ECLIPSE TE 2000S. The area of the scratches was measured and quantified using ImageJ Analysis software. The cell migration across the wounds was expressed as the percentage of wound closure. The experiments were repeated three times and representative photographs are shown.

Cell cycle analysis by flow cytometry

For fluorescence-activated cell sorting (FACS) analysis, HN13 cells were plated at a density of 10000 cells per 100 mm dish in DMEM supplemented with 10% FBS. Twenty-four hours after plating, the cells were treated with vehicle or UVB1 (100 nM) during 120 h. After the indicated time, the cells were harvested by trypsinisation, washed twice with ice-cold 1× PBS, fixed by drop-wise addition of 70% ethanol (approximately 1×10^6 cells/mL), and incubated at 4°C during 24 h. Before flow cytometry analysis, the cellular double-stranded nucleic acids were stained with propidium iodine (Roche, 50 μg/mL) and RNase A (100 U/mL) to degrade double stranded RNA in PBS for 20 min at room temperature. Cell cycle analysis was performed with FACScan flow cytometry (Becton Dickinson). Data were analysed using CellQuest software (Becton Dickinson, Heidelberg, Germany). One thousand forward scatter gated events were collected per sample.

Western blot analysis

Preparation of cell lysates: HN13 and U251 cells were incubated with UVB1 and vehicle (100 nM) for a period of 12 h. Lysates were prepared to examine the expression of VDR, Cyclin D1, p27 and Bax. HN13 y U251 cells were washed twice with PBS and then lysed in lysis buffer containing 2% TRIS 1 M, 1% Triton-X 100, 0.5 M EDTA 0.5 M, 2% sodium chloride 1 M and inhibitors proteins. After 30 min of incubation on ice, the protein content was determined by Bradford assay with bovine serum albumin as standard by Jasco V-630 spectrophotometer and then lysates were stored at −20°C until analysis.

The same amount of protein was run in 15% gel acrylamide-bisacrylamide and transferred to nitrocellulose membranes (PDVF, Millipore). They were blocked for 30 min at room temperature in 5% skim milk. The primary antibodies against VDR (1:750; Santa Cruz Biotechnology), Cyclin D1 (1:1000; Thermo Scientific), p27 (1:500; BD), Bax (1:100; Santa Cruz Biotechnology) and Actin (1:1000; Sigma) were detected by incubating the transferred membrane overnight at 4°C, washing and incubating with the appropriate HRP-conjugated secondary antibodies (Santa Cruz Biotechnology) for 1 h at room temperature. Protein bands were visualised using the enhanced chemiluminescence method. Relative protein levels were calculated by normalisation to the amount of actin protein. Data shown are representative of three independent experiments.

Blood calcium levels

Inbred normal CF1 male mice aged 8–10 weeks and weighing 40 g were obtained from the animal facility of the Departamento de Biología, Bioquímica y Farmacia de la Universidad Nacional del Sur (Bahía Blanca, Argentina) and treated in accordance with the institutional animal care and use committee guidelines. Mice were housed in sterilised cages and provided with filtered water and a standard powdered rodent diet ad libitum. Experimental protocols were initiated following a 7 day acclimatisation period. Calcium level studies were performed following a daily intraperitoneal injection of 5 μg/kg body weight of calcitriol, UVB1 or vehicle ($n = 5$/group). Blood samples were collected from mice (basal levels as well as 24, 48, 72 and 96 h post injection). Animals were anesthetised with Acedan® (Holliday Scott, Argentina), 0.22 mg/kg body weight; heparinised capillary tubes were used to collect blood from the retro-orbital sinus. Samples were held on ice, processed at 4°C, and plasma was separated by centrifugation at 13000 rpm and stored at −20°C until assayed. Approximately 10–30 μL of plasma/mouse was obtained each time. Calcium concentration was determined using Ca-Color Arsenazo III AA kit (Wiener Lab, Argentina), measuring the absorbance at 650 nM; the sample calcium concentration was calculated based upon calcium standards provided by the manufacturer. Additionally, the haematocrit for each mouse was analysed before and following

treatments at 24, 48, 72 and 96 h to determine if the mice were healthy.

To test the effect on plasma calcium levels of a higher dose of the UVB1 analogue (40 μg/kg body weight) we used male, athymic nude mice (N:NIH(S)-*Fox1*^{nu}; Facultad de Ciencias Veterinarias de la Universidad Nacional de La Plata, Argentina), five animals per condition, 20 g of weight and 8 weeks of age. Animals were maintained in a specific pathogen-free environment under controlled conditions of light and humidity for several weeks and treated in accordance with the institutional animal care and use committee guidelines. UVB1 and vehicle were administrated by an injection three times a week during a total period of 21 days. General toxicity was assessed by clinical measures, such as weight loss, changes in appearance and behaviour, lethargy and death. Animal weight was evaluated three times a week. Blood samples were collected from mice at the end of the treatment period and plasma calcium levels were performed as previously described.

Liver and kidney histological analysis

Dissected livers and kidneys from animals treated with UVB1 and vehicle at 40 μg/kg body weight were fixed in 10% saline formalin during 24 h and gradually dehydrated using serial ethanol concentrations of 70, 90 and 100%. Dehydrated organs were cleared 2 h using xylol and then included in paraffin. Sections (5 μm thick) were prepared using a rotary microtome (Leica, RM 2155), and were attached to clean slides and stained with hematoxylin-eosin for histological examination by an expert pathologist. For each slide, 10 fields at ×100 and ×400 magnification were analysed.

Statistical analyses

GraphPad Prism 5.0 software package was used for all statistical analyses. Cellular counting data were analysed using two-way analysis of variance (ANOVA) followed by one-way ANOVA to determine the effects of increasing concentrations of calcitriol, UVB1 or vehicle on cell number. Bonferroni post test was used to determine statistical significance between sample sets. Differences in CYP24A1 mRNA expression between UVB1, calcitriol and vehicle were analysed for statistical significance using the Student *t*-test. Wound healing areas were analysed by two-way ANOVA and Bonferroni post test. Plasma calcium levels at 5 and 40 μg/kg body weight were evaluated by Student *t*-test. Values of $p < 0.05$ were considered statistically significant for all statistical analyses.

This work was supported by grants from CONICET, ANPCyT and from the Technical Secretary of the Universidad Nacional del Sur and from Xunta de Galicia (CN 2012/184). M.J.F. and M.E.F. are recipients of fellowships from CONICET. We thank Dr. J. Arévalo for kindly analyzing the histological slides.

The authors declare that there are no conflicts of interest.

References

[1] G. Eelen, L. Verlinden, P. De Clercq, M. Vandewalle, R. Bouillon, A. Verstuyf, *Anticancer Res.* **2006**, *26*, 2717–2721.
[2] T. M. Beer, A. Myrthue, *Mol. Cancer Ther.* **2004**, *3*, 373–381.
[3] D. Trump, J. Muindi, M. Fakih, W. Yu, C. Johnson, *Anticancer Res.* **2006**, *26*, 2551–2556.
[4] G. C. Van den Bemd, H. A. Pols, J. C. Birkenhäger, J. P. Van Leeuwen, *Proc. Natl. Acad. Sci. USA* **1996**, *93*, 10685–10690.
[5] Y. Bury, D. Ruf, C. M. Hansen, A. M. Kissmeyer, L. Binderup, C. Carlberg, *J. Invest. Dermatol.* **2001b**, *116*, 785–792.
[6] G. Tocchini-Valentini, N. Rochel, J. M. Wurtz, A. Mitschler, D. Moras, *Proc. Natl. Acad. Sci. USA* **2001**, *98*, 5491–5496.
[7] M. R. Uskokovic, A. W. Norman, P. S. Manchand, G. P. Studzinski, M. J. Campbell, H. P. Koeffler, A. Takeuchi, M. L. Siu-Caldera, D. S. Rao, G. S. Reddy, *Steroids* **2001**, *66*, 463–471.
[8] M. Herdick, Y. Bury, M. Quack, M. Uskokovic, P. Polly, C. Carlberg, *Mol. Pharmacol.* **2000**, *57*, 1206–1217.
[9] A. W. Norman, P. S. Manchand, M. R. Uskokovic, W. H. Okamura, J. A. Takeuchi, J. E. Bishop, J. I. Hisatake, H. P. Koeffler, S. Peleg, *J. Med. Chem.* **2000**, *43*, 2719–2730.
[10] H. Jin, Lee, A. Wislocki, C. Goodman, Y. Ji, R. Ge, H. Maehr, M. Uskokovic, M. Reiss, N. Suh, *Mol Pharmacol.* **2006**, *69*, 1840–1848.
[11] Y. Fall, G. Gómez, M. Pérez, Z. Gándara, X. Pérez, G. Pazos, G. Kurz, WO 2011121152, **2011** [*Chem. Abstr.* **2011**, *155*, 536338].
[12] Z. Gándara, M. L. Rivadulla, M. Pérez, G. Gómez, Y. Fall, *Eur. J. Org. Chem.* **2013**, 5678–5682.
[13] S. Müller, B. Liepold, G. J. Roth, *J. Bestman. Synlett* **1996**, 521–522.
[14] P. S. Manchand, G. P. Yiannikouros, P. S. Belica, P. Madan, *J. Org. Chem.* **1995**, *60*, 6574–6581.
[15] G. H. Posner, J. K. Lee, M. C. White, R. H. Hutchings, H. Dai, J. L. Kachinski, P. Dolan, T. W. Kensler, *J. Org. Chem.* **1997**, *62*, 3299–3314.
[16] A. Mouriño, M. Torneiro, C. Vitale, S. Fernández, J. Pérez-Sestelo, S. anne, C. Gregorio, *Tetrahedron Lett.* **1997**, *33*, 4713–4716.
[17] A. R. Daniewski, L. M. Garofalo, S. D. Hutchings, M. M. Kabat, W. Liu, M. Okabe, R. Radinov, G. P. Yiannikour, *J. Org. Chem.* **2002**, *67*, 1580–1587.
[18] A. J. Brown, E. Slatopolsky, *Mol. Aspects Med.* **2008**, *29*, 433–452.
[19] D. L. Trump, K. K. Deeb, C. S. Johnson, *J. Cancer* **2010**, *16*, 1–9.
[20] G. Jones, D. E. Prosser, M. Kaufmann, *J Lipid Res.* **2014**, *55*, 13–31.

[21] J. Moreno, A. V. Krishnan, D. J. Feldman, *J. Steroid Biochem. Mol. Biol.* **2005**, *97*, 31–36.
[22] K. Yasuda, S. Ikushiro, M. Kamakura, M. Takano, N. Saito, A. Kittaka, T. C. Chen, M. Ohta, T. Sakaki, *J. Steroid Biochem. Mol. Biol.* **2013**, *133*, 84–92.
[23] H. C. Horváth, Z. Khabir, T. Nittke, S. Gruber, G. Speer, T. Manhardt, E. Bonner, E. J. Kallay, *J. Steroid Biochem. Mol. Biol.* **2010**, *121*, 76–79.
[24] V. Petit, B. Boyer, D. Lentz, C. E. Turner, J. P. Thiery, A. M. Valles, *J. Cell Biol.* **2000**, *148*, 957–970.
[25] H. A. P. Pols, J. C. Birkenhäger, J. A. Foekens, J.P.T.M. van Leeuwen, *J. Steroid Biochem. Mol. Biol.* **1990**, *37*, 873–876.
[26] K. C. Chiang, C. N. Yeh, J. T. Hsu, T. S. Yeh, Y. Y. Jan, C. T. Wu, H. Y. Chen, S. C. Jwo, M. Takano, A. Kittaka, H. H. Juang, T. C. Chen, *Cell Cycle* **2013**, *12*, 1316–1325.
[27] E. Eltsner, S. M. Linker-Isreali, J. Said, T. Umiel, S. De Vos, I. P. Shintaku, D. Heber, L. Binderup, M. Uskokovic, H. Koeffler, *Cancer Res.* **1995**, *55*, 2822–2830.
[28] K. C. Chiang, C. N. Yeh, S. C. Chen, S. C. Shen, J. T. Hsu, T. S. Yeh, J. H. Pang, L. J. Su, M. Takano, A. Kittaka, H. H. Juang, T. C. Chen, *Evid. Based Complement Alternat. Med.* **2012**, *2012*, 310872.
[29] K. Satake, E. Takagi, A. Ishii, Y. Kato, Y. Imagawa, Y. Kimura, M. Tsukuda, *Auris Nasus Larynx* **2003**, *30*, 403–412.
[30] C. Gedlicka, G. Hager, M. Weissenböck, W. Gedlicka, B. Knerer, J. Kornfehl, M. Formanek, *J. Oral Pathol. Med.* **2006**, *35*, 472–478.
[31] B. W. Light, W. D. Yu, M. C. Mc, Elwain, D. M. Russell, D. L. Trump, C. S. Johnson, *Cancer Res.* **1997**, *57*, 3759–3764.
[32] J. R. Muindi, R. A. Modzelewski, Y. Peng, D. L. Trump, C. S. Johnson, *Oncology* **2004**, *66*, 62–66.
[33] J. R. Muindi, W. D. Yu, Y. Ma, K. L. Engler, R. X. Kong, D. L. Trump, C. S. Johnson, *Endocrinology* **2010**, *151*, 4301–4012.
[34] T. Kumagai, J. O'Kelly, J. W. Said, H. P. Koeffler, *J. Natl. Cancer Inst.* **2003**, *95*, 896–905.
[35] J. Prudencio, N. Akutsu, N. Benlimame, T. Wang, Y. Bastien, R. Lin, M. J. Black, M. A. Alaoui-Jamali, J. H. White, *J. Natl. Cancer Inst.* **2001**, *93*, 745–753.
[36] D. G. Salomón, S. M. Grioli, M. Buschiazzo, E. Mascaró, C. Vitale, G. Radivoy, M. Pérez, Y. Fall, E. A. Mesri, A. C. Curino, M. M. Facchinetti, *ACS Med. Chem. Lett.* **2011**, *2*, 503–508.
[37] C. Spina, V. Tangpricha, M. Yao, W. Zhou, M. M. Wolfe, H. Maehr, M. Uskokovic, Adorini, L. M. F. Holick, *J. Steroid Biochem. Mol. Biol.* **2005**, *97*, 111–120.
[38] J. N. Hathcock, A. Shao, R. Vieth, R. Heaney, *Am. J. Clin. Nutr.* **2007**, *85*, 6–18.
[39] U. Windberger, A. Bartholovitsch, R. Plasenzotti, K. J. Korak, G. Heinze, *Exp. Physiol.* **2003**, *88*, 431–440.
[40] OECD. Repeated dose 28-day oral toxicity study in rodents, guideline 407, the OECD guideline for testing of chemical. **1995**.
[41] K. J. Livak, T. D. Schmittgen, *Methods* **2001**, *25*(4), 402–408.